FACTA UNIVERSITATIS
Series: **Mechanical Engineering** Vol. 2, N^{o} 1, 2004, pp. 109 - 124

PROCESSING THE LIFETIME OF BUCKET WHEEL EXCAVATOR PARTS IN STRIP MINE TECHNOLOGIES [1]

UDC 621.87:622.23.08

Zoran Marinković, Goran Petrović

Mechanical Engineering Faculty, University of Niš
A. Medvedeva 14, 18000 Niš, Serbia and Montenegro

Abstract. *The paper presents a complex model of calculating the parts of complex machine systems exposed to variable load and strain. This model includes calculation of operational safety and lifetime of parts, on the example of the bucket wheel excavator driving mechanism. The goal is to apply this calculation model to making safe and reliable machine systems, i.e. bucket wheel excavators, which will operate efficiently under complex exploitation conditions in coal mines.*

Key Words: *Bucket Wheel Excavator, Load, Operational Stress, Discretization, Lifetime*

1. INTRODUCTION

A large number of complex machine systems (MS) operate under highly variable exploitation conditions. For this reason, their component parts are exposed to variable load, i.e. strain, which is usually random. In exploitation, it is required that each MS has a certain operational safety and reliability for the given lifetime. However, as a result of the effect of variable strain with sufficient intensity and duration, some parts may be damaged, and failures may occur. Failures, i.e. damage of parts, are manifested as excessive or permanent deformation, static or violent fracture, dynamic fracture caused by fatigue, increased wear, corrosion, overheating, etc.

The modern concept of calculating these complex MS involves making a complex calculation model. This model should cover checking the relevant failures, i.e. calculation-based determination or assessment of the safety, lifetime, and reliability of component parts and the system as a whole, on the basis of real MS exploitation conditions.

The paper describes a calculation model of this type on the example of the bucket wheel excavator as a complex MS for operation in coal strip mines. A particular treatment

Received November 26, 2003

[1] The paper was written within the project 'Development of MIN-ENGINEERING products on the basis of software for structural analysis' from Program of Technological Development, No. MIS. 3.07.0082, financed by Ministry of Science and Environmental Protection of Republic of Serbia.

is given to the bucket wheel driving mechanism, whose vital parts are used to check the safety and lifetime on the basis of real exploitation conditions. This is done by employing analytical modeling procedures within a simulation model with originally developed computer programs. The goal is to fabricate highly efficient bucket wheel excavators in the phase of modular and variant design of these machine systems; their reliable operation supports gives support to energy efficiency of the country [1, 2].

2. Description of the Complex Model of Calculating the Bucket Wheel Driving Mechanism

The bucket wheel excavator is a complex machine with mining technology within modern technology of coal strip mining. It consists of a complex spatial structure, several driving mechanisms, and the control mechanism (Fig. 1). The most peculiar among these mechanisms is the bucket wheel drive, located on top of the arrow. Figure 2 shows the kinematic scheme of the bucket wheel driving mechanism in excavator SRs 470.20.3 LAUHAMER, consisting of a motor (1), elastic coupling with a brake (2), four-step reduction gear (3) with a lamellar coupling (4) on the second shaft of the reduction gear, and the bucket wheel (5) with 8 buckets [1].

Fig. 1. Bucket Wheel Excavator

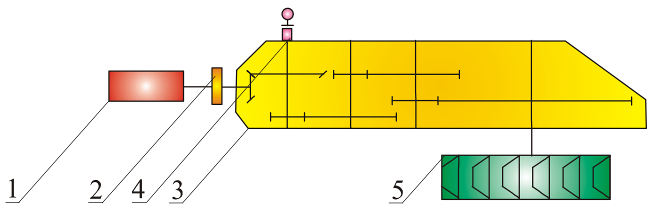

Fig. 2. Scheme of the Bucket Wheel Driving Mechanism

The process of direct digging by the bucket wheel excavator is realized in a combination of continual rotation of the bucket wheel in the vertical, and arrow movement in the horizontal plane. As a result of the drive's performances, characteristics of the soil, and inequality of digging resistances on the buckets, the bucket wheel excavator is subject to a number of external loads changing dynamically and randomly. As a consequence, the vital parts of the excavator's structure and driving mechanisms are exposed to a variable load which, when it exceeds critical values, causes damage and delay in the operation of the entire system.

An adequate design of bucket wheel excavators requires the application of a complex analytical model for calculating its vital parts, which consists of several steps [2]:

- modeling the bucket wheel driving mechanism in order to choose an equivalent and mathematical model adequate to its characteristics,
- simulating the operation of the driving mechanism in order to determine the functions of operational loads and strains of vital parts for characteristic bucket wheel excavator's operation modes,
- discretizing the functions of operational stresses in order to obtain corresponding characteristics and their spectrums, required for calculation, and,
- calculating operational safety and lifetime of vital parts for certain types of strain in order to prevent their destruction and failure.

3. Modeling the Bucket Wheel Driving Mechanism

In this case, modeling means substitution of a complex real system, i.e. the bucket wheel driving mechanism (Fig. 2) with the corresponding equivalent dynamic and analytical model. Research of this issue has shown that this complex real system is successfully replaced by the torsional elasto-kinetic model with a finite number of discrete rotary masses and elastic bonds between them. The masses are defined by moments of inertia J_i, and the bonds by coefficients of rigidity c_i and damping b_i. However, suitable reduction of these characteristics reduces the complex equivalent dynamic model to a very simple one, with only two rotary masses and one elastic bond (Fig. 3) [2, 3, 4, 5]. This model can yield results relevant for analyzing the operation and calculating this mechanism.

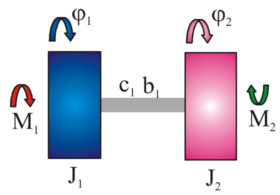

Fig. 3. Equivalent Torsional Elasto-kinetic Model with Two Rotary Masses

For the concrete example, the characteristics of the equivalent model during reduction at the reduction gear's input – referent shaft (Fig. 3), are: J_1 = 17.2 kgm^2, J_2 = 6.25 kgm^2, c_1 = 86210 Nm and b_1 = 14.00 Nms.

The masses of the model in Fig. 3 in bucket wheel operation, with 8 buckets and diameter D_{RT}, under the effect of disturbing moments from motor $M_1 = M_M$ and digging resistance $M_2 = -M_W$, are in forced damped oscillatory motion. It is for this reason that the mathematical model describing this motion is given through the system of two non-homogenous differential equations of the order of two [2, 3, 4]:

$$\begin{aligned} J_1\ddot{\varphi}_1 + b_1(\dot{\varphi}_1 - \dot{\varphi}_2) + c_1(\varphi_1 - \varphi_2) = M_1 = M_M = f(\dot{\varphi}_1) \\ J_2\ddot{\varphi}_1 - b_1(\dot{\varphi}_1 - \dot{\varphi}_2) - c_1(\varphi_1 - \varphi_2) = M_2 = -M_W = -F_t(\psi)\cdot D_{RT}/2 \end{aligned}, \tag{1}$$

where, apart from the values which have already been explained, $\varphi_j, \dot{\varphi}_j, \ddot{\varphi}_j$ - coordinates of the angle, angular velocity, and angular acceleration of the driving (i = 1) and driven (i = 2) masses, are generated.

The characteristic of starting motor $M_1 = M_M = f(n) = f(\dot{\varphi} = \pi\, n/30)$ is modeled by observing its two intervals separately (Fig. 4): from initial moment M_p to maximal M_m and from maximal M_m to nominal M_n. The first interval can be defined by a polynomial of the fourth order, while the second is best described by the so-called Clos's equation. The complete procedure of modeling this characteristic is performed in MatLab software package, with graphical representation in Simulink module, as given in Fig. 4. [3, 4].

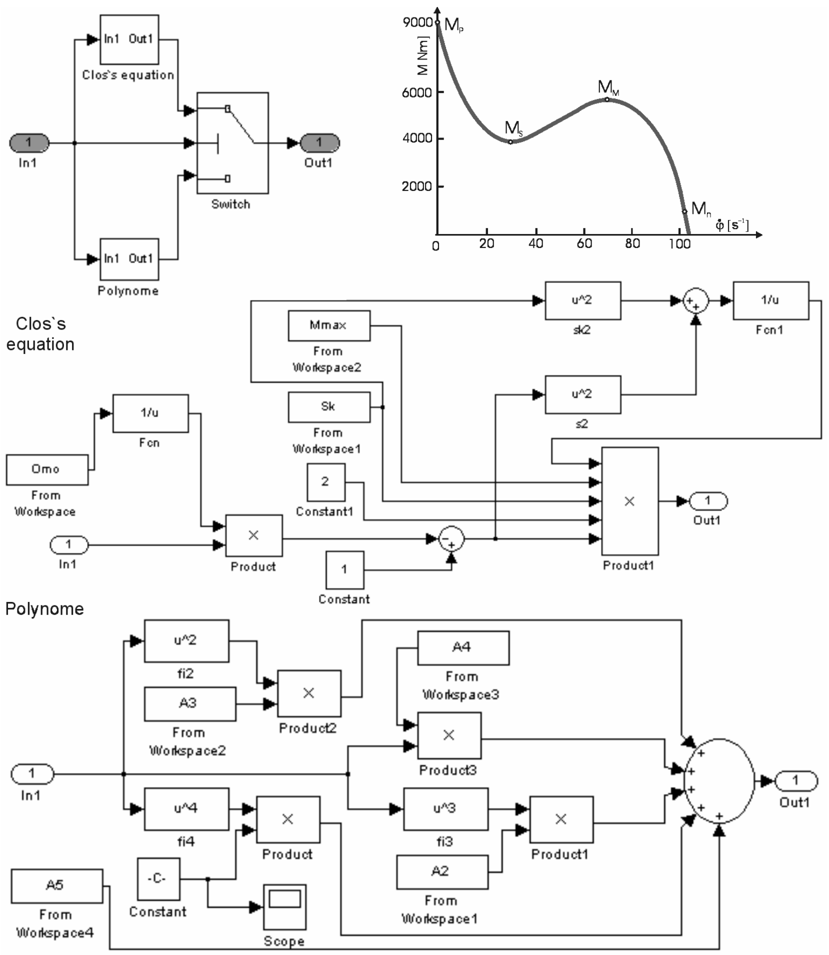

Fig. 4. Modeling the Motor Starting Curve

The disturbing moment on the second - driven mass, i.e. on the bucket wheel with 8 buckets, $M_2 = -M_W = -F_t(\psi) \cdot D_{RT} / 2$ depends on digging resistance, i.e. tangential component $F_t(\psi)$ and bucket wheel diameter D_{RT}. Digging resistance can be represented as multiplication of specific linear digging resistance k_l (characteristics of the soil) and mean sum of the length of cutting edges l_{sr}. The relatively good accuracy of change in tangential force on the buckets which are at that moment in the process of digging is given by the following relation [3, 4]:

$$F_t(\psi) = k_l \cdot l_{sr} \cdot f_o(\psi)\,, \quad f_o(\psi) = \begin{cases} \sin\psi & 0 \le \psi \le \pi/2 \\ (\alpha - \psi)/(\alpha - \pi/2) & \pi/2 \le \psi \le \alpha \\ 0 & \psi > \alpha \end{cases} \tag{2}$$

This discussion can be used as the basis for simulating the value of specific digging resistance by using the modules from MatLab software package. This module is relatively simple to use, as it automatically generates a string of random numbers according to the pre-given distribution and sample size. Having thus obtained the values of specific digging resistance and assumed active length of cutting edges, we proceed to the block-scheme of Simulink module for generating digging resistance of a single bucket. The final step implies the summing up of individual resistances in order to obtain total digging resistance (Fig. 5) [3, 4].

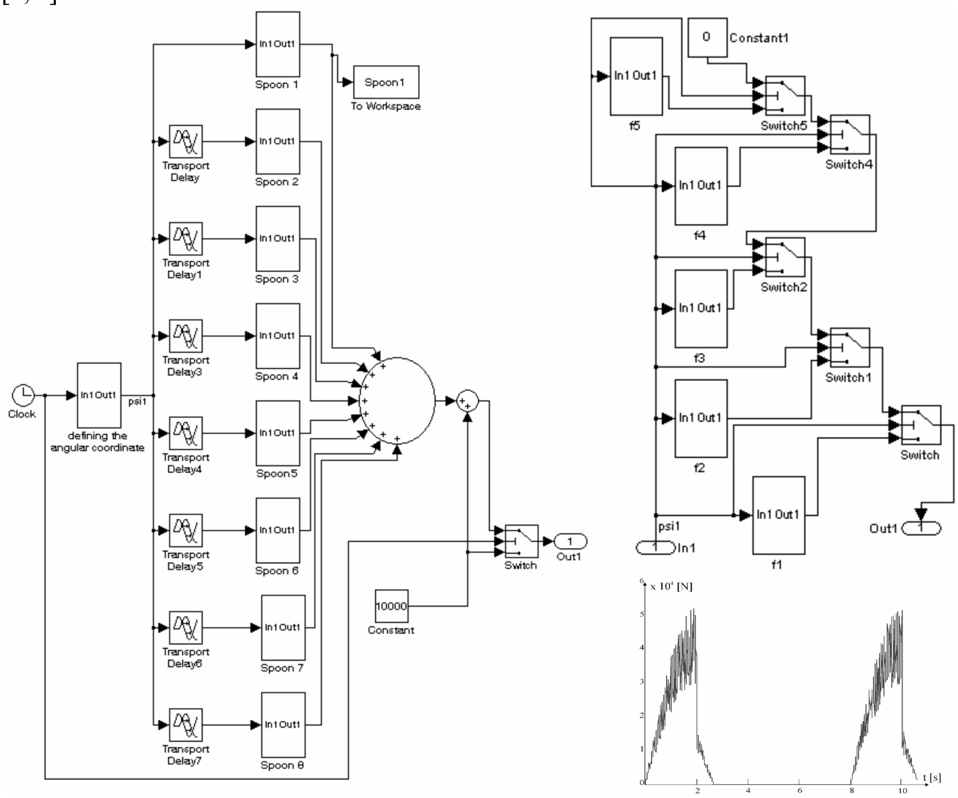

Fig. 5. Modeling Total Digging Resistances and Resistance on a Single Bucket

4. Simulating the Operation Of The Bucket Wheel Driving Mechanism

Simulation means a procedure for imitation and analysis of a real system's operation by means of its dynamic and mathematical model. By solving the system of differential equations (1) for defined disturbing moments ($M_1 = M_M$ and $M_2 = -M_W$) and initial conditions, the example of the bucket wheel driving mechanism is used to obtain the laws of motion of the first – driving mass $\varphi_1(t)$ and the second – driven mass $\varphi_2(t)$ of the model in Fig. 3 [4].

On the basis of these laws of motion, it is easy to determine deformation of elastic bond $\Delta\varphi(t) = \varphi_1(t) - \varphi_2(t)$, i.e. change in the torsional moment of the referent shaft, as:

$$M_t(t) = T(t) = c_1 \cdot \Delta\varphi(t) = c_1 \cdot (\varphi_1(t) - \varphi_2(t)) . \tag{3}$$

For the concrete example of the bucket wheel driving mechanism in excavator SRs 470.20.3 LAUHAMER, MatLab program package and its Simulink module were used to obtain change in the torsional moment of the driving shaft $M_t(t) = T(t)$ (Fig. 6). This change lasts 30s, of which the first 5s belong to the period of acceleration of bucket wheel rotation without digging.

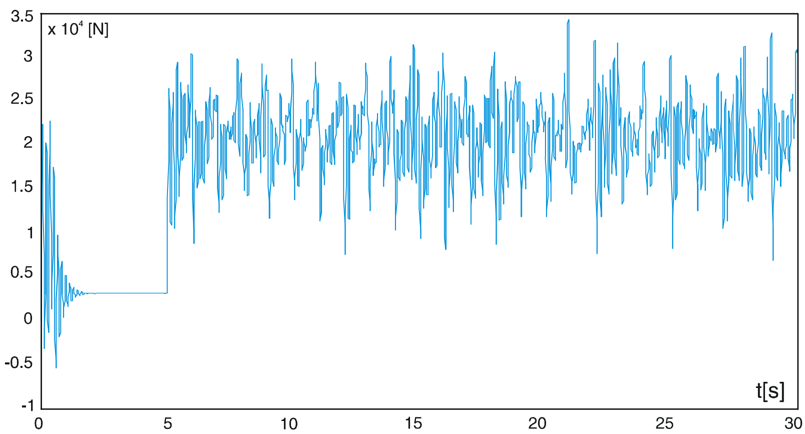

Fig. 6 Change in the Torsional Moment $M_t(t) = T(t)$ of the Mechanism's Driving Shaft

Apart from torsional moment $M_t(t) = T(t)$, the driving mechanism's referent shaft at cogwheels is also loaded by cross forces: tangential $F_t(t)$, radial $F_r(t)$ and axial $F_a(t)$ in corresponding planes, in the way shown in Fig. 7a. These forces, which cause bending of the shaft, depend on the torsional moment $M_t(t) = T(t)$ and cogwheel dimensions.

These external loads, in the form of torsional moment $M_t(t) = T(t)$ and cross forces $F_t(t)$, $F_r(t)$ and $F_a(t)$ cause the shaft's corresponding complex strain, i.e. cause the occurrence of tangential torsional stresses $\tau_t(t)$ and orthogonal bending stresses $\sigma_f(t)$. As can be seen, these operational stresses are time functions and are determined by means of known expressions from the resistance of materials at certain characteristic points of the shaft.

The time function of shaft torsion $\tau_t(t)$, which is concurrent with change in torsional moment $M_t(t) = T(t)$, can be written in the following form:

$$\tau_t(t) = M_t(t)/W_0 = T(t)/W_0 = 16 \cdot T(t)/(\pi \cdot d_v^3) . \tag{4}$$

where W_0 = W_p - is polar moment of inertia of the shaft's cross section with diameter d_v.

The function of bending the shaft $\sigma_f(t)$ is not concurrent with change in torsional moment $M_t = T(t)$. The way in which this force is determined in loading the shaft by forces $F_t(t)$, $F_r(t)$ and $F_a(t)$ and moments $M_x(t)$, $M_y(t)$ and $M(t)$ in function $T(t)$, is given in Fig. 7b. Due to shaft torsion, the position of the edge point of the section changes in relation to the neutral axis between maximal value in zones of pressure and straining according to law $(t) = (d_v/2)\cdot\sin\varphi(t)$, as shown in Fig. 7a. The analytical expression for the function of the shaft's bending stress $\sigma_s = \sigma_f(t)$ will be:

$$\sigma_f(t) = M(t)\cdot y(t)/I_x = M(t)\cdot(1/W_x)\cdot\sin(\varphi(t)+\varphi_0) \quad , \tag{5}$$

where: $I_x = \pi\cdot d_v^4/64$, $W_x = \pi\cdot d_v^3/32$ - are moment of inertia and axial resistance moment of the shaft's cross section with diameter d_v.

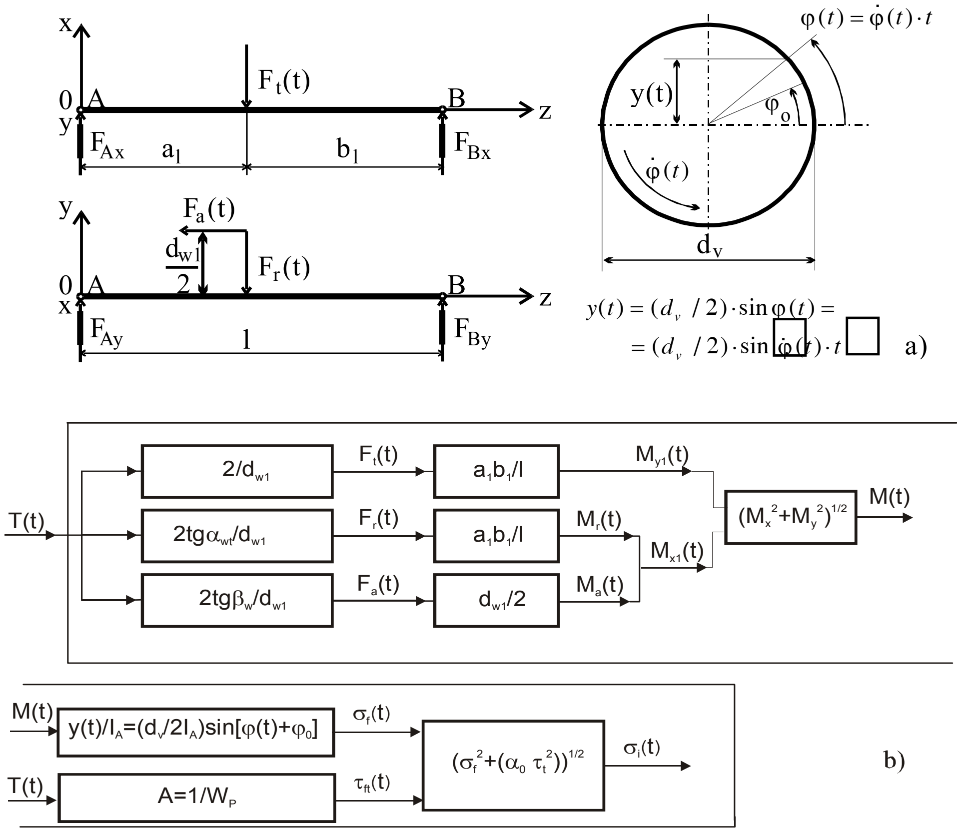

Fig. 7. Scheme of Loading the Shaft by Cross Forces (a) and Calculation of Equivalent Operational Stress (b)

As in this case expression $y(t) / I_x = (1 / W_x) \cdot \sin(\varphi(t) + \varphi_0)$ is a function of time, then change in bending moment $\sigma_f(t)$ also depends on both function of load $M_t = T(t)$, i.e. $M_s = M_i(t)$, and position of the edge fiber $y(t)$ and initial angle φ_0.

According to the hypothesis on equivalent stress at complex straining, the total stress will be:

$$\sigma_i(t) = \sqrt{\sigma_f^2(t) + (\alpha_0 \cdot \tau_t(t))^2}\ , \tag{6}$$

where $\alpha_0 = \sigma_{Df(-1)} / \tau_{Dt(0)}$, and $\sigma_{Df(-1)}$ denotes permanent dynamic endurance of the material from which the shaft is made at randomly varying bending, while $\tau_{Dt(0)}$ denotes permanent dynamic endurance at unidirectional variable torsion.

Figure 8 shows change in the functions of operational stresses of torsion $\tau_t(t)$ (4), bending $\sigma_f(t)$ (5) and total strain $\sigma_i(t)$ (6), obtained by analyzing the concrete example through simulation by means of MatLab program package and its sub-program Simulink.

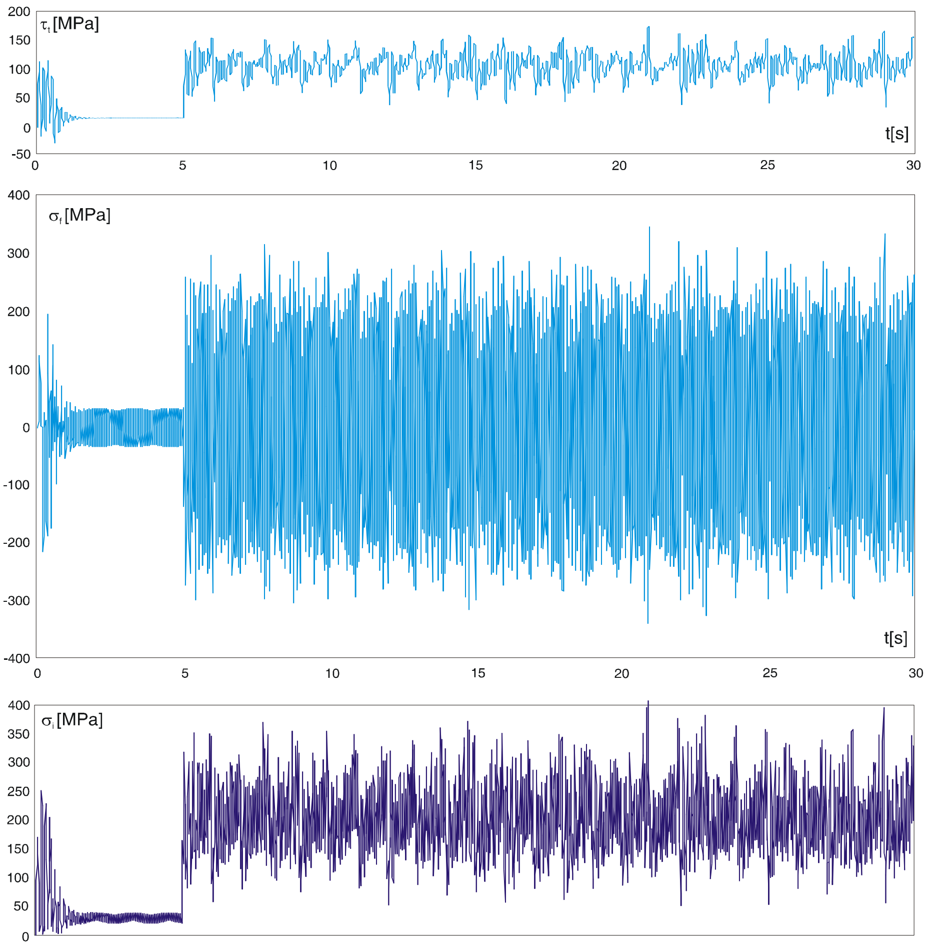

Fig. 8. Change in the Functions of the Shaft's Operational Stresses $\sigma_f(t)$, $\tau_t(t)$ and $\sigma_i(t)$

5. DISCRETIZING THE FUNCTIONS OF OPERATIONAL STRESSES AND THEIR SPECTRUMS

The obtained functions of operational stresses reflect their character of change, and relevant parameters (features) for further calculation. Such parameters are maximal values of operational stresses σ_{max} which may cause a violent fracture or deformation of parts, as well as variable amplitudes σ_{ai} and mean values σ_{mi} , which also contribute to fatigue breakdown of parts, etc.

To separate these features, methods of discretization and statistical processing are employed in order to obtain so-called spectrums of operational stresses. In this case, spectrum means a simplified representation of the results of statistical processing for separated features of operational stresses as a function of distribution. In this way, the history of operational stress occurrence is lost, and a simpler set of relevant features for further calculation of parts is formed. Broadband functions $\tau_t(t)$ (Fig. 8a) require bi-parameteric discretization of the distribution of amplitudes and mean values $f(\sigma_a, \sigma_m)$, while in narrow-band functions $\sigma_f(t)$ (Fig. 8b) uni-parameteric discretization yields only the distribution of amplitudes $f(\sigma_a)$ [5].

The essence of this statistical processing lies in variability of operational stresses and their features' property of dispersion. Apart from the function of distribution – density, these spectrums are often given in the form of cumulative declining distribution with logarithmic division, as such a form is comparative with Wöhler's curves of parts' material fatigue. There is a large number of methods - procedures for separating, counting, and classifying features of the functions of operational stresses, which can be classified into several groups. However, the preferred method today is the cycle method, i.e. its popular variant - Rain Flow Method [5, 6].

The originally developed computer program 'SPECTRUM' [5], which, apart from other things, employs the cycle method, was used to process broadband change in complex stress $\sigma_i(t)$ by bi-parametric discretization (Fig. 8c). In this type of change, the number of extreme values is $N_{ext} = 1868$, and maximal, i.e. minimal value, is: $\sigma_{max} = 408.73$ MPa and $\sigma_{min} = 0$ MPa (1 MPa = 10 kN/cm^2). Variational strings of amplitudes $\sigma_a = 0 \div 210$ MPa and mean values $\sigma_m = 10 \div 340$ MPa separated by bi-parametric discretization, are divided into 10 classes with widths $\Delta\sigma_a = 21$ MPa and $\Delta\sigma_m = 34$ MPa. Statistical processing of these strings results in the following Table 1 for the seventh class of mean values $\sigma_m = 225$ MPa.

Table 1. Results of Processing a Random Process

Classes No	σ_{ai} *MPa*	n_i	n_{uki}	$f_i = \frac{n_i}{n_{uk}}$	F_i	H_i	$H_i \cdot n_b$	$\log(H_i \cdot n_b)$
1	0 ÷ 21	0	0	0	0	1	1000000	6
2	21 ÷ 42	31	31	0,1245	0,1245	0,8755	875500	5,9423
3	42 ÷ 63	141	172	0,5663	0,6908	0,3092	309200	5,4903
4	63 ÷ 84	32	204	0,1285	0,8193	0,1807	180700	5,2570
5	84 ÷ 105	19	223	0,0763	0,8956	0,1044	104400	5,0188
6	105 ÷ 126	12	235	0,0482	0,9438	0,0562	56200	4,7499
7	126 ÷ 147	10	245	0,0402	0,9839	0,0161	16100	4,2059
8	147 ÷ 168	3	248	0,0012	0,9960	0,0040	4000	3,6038
9	168 ÷ 189	1	249	0,0040	1	0	0	-
10	189 ÷ 210	0	249	0	1	0	0	-

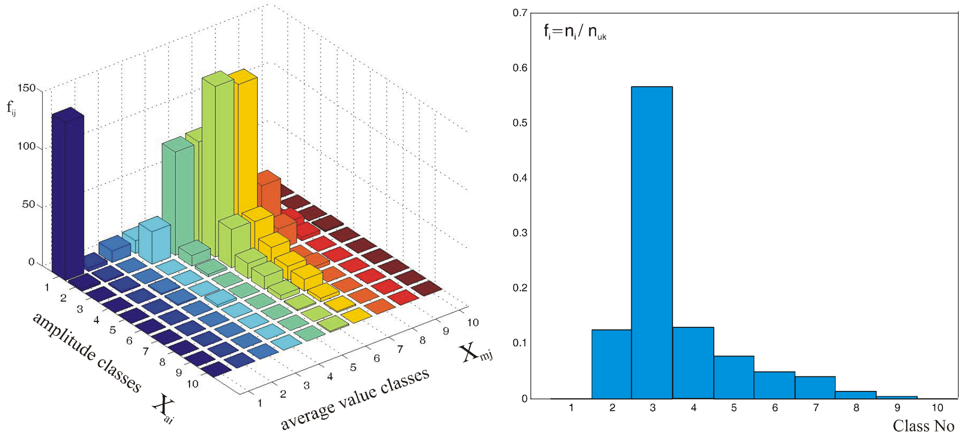

Fig. 9. Frequency Stereogram and Histogram of the Seventh Class of Mean Values

Fig. 9a shows the stereogram as a graphical interpretation of statistical processing $f(\sigma_a,\sigma_m)$. From it, it is relatively simple to obtain the histogram of amplitude change for a pre-given constant mean value σ_m = 225 MPa, (Fig. 9b), as shown in Table 1.

6. Calculation of Operational Safety and Lifetime of Parts

The final step in the complex model for calculating vital parts of the bucket wheel driving system includes the determination of their safety and lifetime. One of the criteria of choosing the shape and dimensions of parts is that operational stresses should be below the values leading to critical states (deformation, fracture, and other types of damage), whereby the material which is used should be used rationally. In practical calculations, these critical and operational stresses are compared. A properly dimensioned part requires that critical stresses should be larger than operational ones in order to ensure operational safety and reliability for a given lifetime.

Critical states, i.e. critical stresses, are characteristic for the material of which these parts are made. They are obtained experimentally by examining so-called standard test specimens or model parts for certain types of strain by a standard procedure on adequate machines. Information about material characteristics can be found in technical literature.

A large number of methods and procedures for calculating machine parts is used today; their development is determined by the development of more accurate theoretical and experimental methods of determining operational and critical stresses. The practical application of these methods depends on a number of criteria, which can, in general, be divided into several groups, according to:

- design phase into preceding and final,
- type of change of operational stresses into static and dynamic, and,
- character of input and output calculation values into deterministic and probabilistic, etc.

A concrete example of checking the referent shaft of the bucket wheel driving mechanism involves final calculations of operational safety and lifetime for a dynamic change of operational stresses within deterministic calculations. As in this case time functions of operational stresses are given (Fig. 8), which can be used to easily determine their maximal values, the shaft's operational safety can also be checked with respect to the static material characteristics.

As has been mentioned, operational safety is checked by comparing critical and operational stresses, i.e. their ratio should be more than one in order to satisfy a standard or desired degree of safety. In general, this is expressed by the following relation:

$$\upsilon = [\sigma_{kr}]/\sigma_r < \upsilon_{doz} \ , \tag{7}$$

where:

- $[\sigma_{kr}]$ – is critical stress as material characteristic which may be the breaking strain $\sigma_M = R_M$, yield strain $\sigma_M = R_M$, dynamic endurance σ_D or σ_A for corresponding type of strain,
- σ_r – operational stress, which may be maximal or amplitude value of corresponding change in operational stresses,
- υ_{doz} – allowed degree of safety.

For example, in the concrete example of bending the shaft made of carbon-structural steel Č 0545 with mechanical characteristics: $\sigma_M = R_M = 600$ MPa and $\sigma_V = R_V = 350$ MPa, for known maximal value of bending stress $\sigma_{\max} = 320$ Mpa (Fig. 8b) the following values of degree of safety are obtained: $\nu_M = \sigma_M/\sigma_{\max} = 600/320 = 1.9$ and $\nu_V = \sigma_V/\sigma_{\max} = 350/320 = 1.1$.

Previous calculations of operational safety have been static, when maximal values of operational stresses $\sigma_{\max}$ were compared with static material characteristics (σ_M and σ_V). They can also be dynamic, when maximal amplitudes $\sigma_{a\max}$ of time change are compared with material endurance σ_D or σ_A. However, it is not always advisable to dimension parts so that maximal operational stress amplitude is below material endurance. This means that the part is dimensioned within permanent dynamic strength so that it will theoretically have unlimited lifetime. For this reason, it is allowed for a certain number of amplitudes to exceed material resistance, which contributes to material fatigue and possible occurrence of cracks and fatigue breakdown. In this case, calculations are performed in the field of operational strength, i.e. what is calculated is the lifetime.

To determine the lifetime of the part for the case given above, we observe Fig. 10. In this figure, what can be seen from the semilogarithmic division stress - number of changes $\sigma - \log N$ is the uni-parametric spectrum of operational stresses - amplitudes, and Wöhler's curve of the part's material fatigue [6, 7].

The given uni-parametric spectrum in Fig. 10 represents a declining step function of the amplitudes of irregular change in operational stresses in the discrete form (σ_{ai}, n_{ib}) and it applies to a certain exploitation period (strain block n_b), repeated λ_r times in the part's total lifetime. The following can be determined for the known parameters of the strain block: total number of changes of all amplitudes in one strain block (n_{uk}), number of amplitude changes σ_{ai} in the i-th degree (n_i) and total number of amplitude changes in all degreed ($1 \div k$) for total lifetime ($N_{uk} = N_r$), respectively, from the following expressions, as:

$$n_{uk} = \sum_{i=1}^{k} n_{ib} = n_b \, , \quad n_i = \lambda_r \cdot n_{ib} \, , \quad N_{uk} = \sum_{i=1}^{k} n_i = \lambda_r \cdot \sum_{i=1}^{k} n_{ib} = \lambda_r \cdot n_b = N_r \, . \tag{8}$$

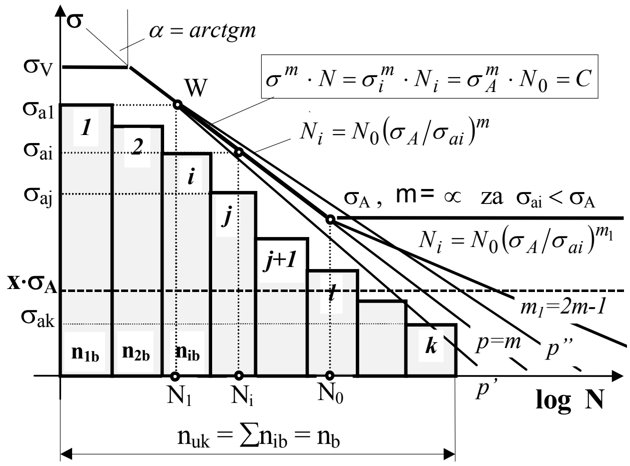

Fig. 10. Calculation of Lifetime of Parts, Wöhler's Curve and Spectrum of Operational Stresses

The equation of Wöhler's curve from Fig. 10 for steels with represented horizontal part to the right of the breaking point is:

$$\begin{array}{llll} \sigma^m \cdot N = \sigma_A^m \cdot N_0 = const. & \text{for} \ \ \sigma \geq \sigma_A & \text{and} & N \leq N_0 \\ N = \infty & \text{for} \ \ \sigma < \sigma_A & \text{and} & N > N_0 \end{array}, \tag{9}$$

where:
σ and N - are current values of stress and number of its changes,
σ_A and N_0 - dynamic endurance and base number of changes, as material characteristics,
m - the exponent defining the left part of Wöhler's curve, and depending on type of element and type of strain.

In spectrum from Fig. 10, a part of amplitudes σ_{ai} from $i = 1 \div j$ exceed σ_A, while the others from $i = j + 1 \div k$ are below σ_A. This means that the first amplitudes can contribute to material fatigue and fracture of the part. In this case, calculation of strength of parts by means of direct comparison of the characteristics of operational stresses σ_{ai} and material σ_A is not possible, as the change in stress is irregular, while the Wöhler's curve is obtained by regular change in strain. For this reason, these types of calculation make use of linear hypotheses on accumulation of damage due to fatigue. Some of these hypotheses are Palmgreen-Miner's (P-M), Corten-Dolan's (C-D), Haibach's (H), Serensen-Kogaev's (S-K) etc [6, 7].

The first hypothesis introduces linear accumulation of damage by those amplitudes of operational stresses which exceed permanent dynamic strength. This is expressed through the following relation [6]:

$$D_{uk} = \sum_{i=1}^{j} D_i = \sum_{i=1}^{j} \frac{n_i}{N_i} \geq 1 \quad \text{for} \quad \sigma_{ai} > \sigma_D \quad (i = 1 \div j), \tag{10}$$

where the new values are:
D_{uk} - total damage as linear sum of partial damages D_i,

N_i - so-called tolerable number of changes the part's material stress according to Wöhler's curve for the corresponding amplitude of operational stresses σ_{ai} (Fig. 10), which is determined from equation (9) as:

$$N_i = \begin{cases} N_0(\sigma_A/\sigma_{ai})^m & \text{for } \sigma_{ai} \geq \sigma_A \quad (i = 1 \div j) \\ \infty & \text{for } \sigma_{ai} < \sigma_A \quad (i = j+1 \div k) \end{cases}. \tag{11}$$

The lifetime of parts expressed in a number of blocks until fatigue breakdown λ_r is obtained when expressions for n_i (8) and N_i (11) are substituted in the relation which determines total damage D_{uk} (10), as in the following:

$$\lambda_r = \sum_{i=1}^{j} \frac{N_0 \cdot (\sigma_A/\sigma_{ai})^m}{n_{ib}} = \frac{N_0 \cdot \sigma_A^m}{\sum_{i=1}^{j} \sigma_{ai}^m \cdot n_{ib}}. \tag{12}$$

In the Palmgreen-Miner's (P-M) hypothesis, the calculated total number of changes in amplitudes of operational stresses until fatigue breakdown N_r, is obtained if in the third expression (8) the expression obtained for λ_r (12), is substituted as:

$$N_r = \lambda_r \cdot n_b = \frac{N_0 \cdot \sigma_A^m \cdot n_b}{\sum_{i=1}^{j} \sigma_{ai}^m \cdot n_{ib}} = \frac{N_0}{(\sigma_{a1}/\sigma_A)^m \cdot \sum_{i=1}^{j} (\sigma_{ai}/\sigma_{a1})^m (n_{ib}/n_b)} = \frac{N_0}{\gamma_p^m \cdot K_N}, \tag{13}$$

where:

$\sigma_{a1} = \sigma_{a\,\max}$ - is maximal amplitude in the spectrum, $\gamma = \sigma_{a1} / \sigma_A$ - overload coefficient, and

$K_N = \sum_{i=1}^{j} (\sigma_{ai}/\sigma_{a1})^m \cdot (n_{ib}/n_b)$ - coefficient of spectrum fullness.

The other hypotheses have been corrected, as they take into account the effect of amplitudes below σ_A on accumulation of fatigue damage. The effect of these amplitudes differs from one hypothesis to another [6, 7]. Thus, the Corten-Dolans (C-D) hypothesis introduces from point W in Fig. 10 a new continual oblique line of fatigue with another exponent $p = K_{CD} \cdot m = (0.7 \div 1.6) \cdot m$ and assumes that all amplitudes σ_{a1} ($i = 1 \div k$) contribute to fatigue.

Haibach (H) introduces a correction in the field of permanent dynamic strength below σ_A to the right of the breaking point in Fig. 10, a new fictive fatigue line with another inclination $m_1 = 2m - 1$. This correction has enabled linear summing of all damages from $i = 1 \div k$ for both parts of the broken fatigue line without discarding small amplitudes.

The Serensen-Kogaev's (S-K) hypothesis introduces the so-called function of interaction $a_p < 1$, which is multiplied by the calculated number of changes N_r (13) obtained from the Palmgreen-Miner's hypothesis.

Finally, the expressions for calculated values of total number of changes N_r, number of blocks λ_r and lifetime T_r (h) until fatigue breakdown can be generalized for all hypotheses as [6, 7]:

$$N_r = \frac{a_p \cdot N_0}{(\sigma_{a1}/\sigma_A)^m \cdot K_N} = \frac{a_p \cdot N_0}{\gamma_p^m \cdot K_N}, \quad \lambda_r = \frac{N_r}{n_b}, \quad T_r = \lambda_r \cdot t_b, \tag{14}$$

where

K_N - is coefficient of the fullness of strain spectrum (block), which, for previously stated corrected linear hypotheses, respectively for hypotheses (C-D), (H) and (S-K and P-M), is:

$$K_N = \sum_{i=1}^{k}\left[\left(\frac{\sigma_{ai}}{\sigma_{a1}}\right)^p \left(\frac{n_{ib}}{n_b}\right)\right] \quad \text{for} \quad \sigma_{ai} > 0 \quad (i = 1 \div k)\,,$$

$$K_N = \sum_{i=1}^{j}\left[\left(\frac{\sigma_{ai}}{\sigma_{a1}}\right)^m \left(\frac{n_{ib}}{n_b}\right)\right] + \gamma_p^{m-1}\cdot\sum_{i=1}^{k}\left[\left(\frac{\sigma_{ai}}{\sigma_{a1}}\right)^{2m-1} \left(\frac{n_{ib}}{n_b}\right)\right] \text{ for } \sigma_{ai} > 0 \quad (i = 1 \div k)\,, \tag{15}$$

$$K_N = \sum_{i=1}^{j}\left[\left(\frac{\sigma_{ai}}{\sigma_{a1}}\right)^m \left(\frac{n_{ib}}{n_b}\right)\right] \quad \text{for} \quad \sigma_{ai} > \sigma_A \quad (i = 1 \div j)\,,$$

a_p - function of interaction, which has values from 0.2 ÷ 1.0 for Serensen-Kogaev's hypothesis, and for the other functions 1.0, and is determined from expressions [6, 7]:

$$a_p = (\xi\cdot\gamma_p - \kappa)/(\gamma_p - \kappa)\,, \quad \kappa = 0{,}5\,, \quad \xi = \sum_{i=1}^{l}(\sigma_{ai}/\sigma_{a1})\cdot(n_{ib}/n_b)\,, \tag{16}$$

$t_b(h)$ - duration of strain block.

Figure 11. shows comparison of the unit spectrum of operational amplitudes from Fig. 9b and Wöhler's curve of amplitude endurance Č 0545. The unit amplitude spectrum, as strain block log ($H_i \cdot n_b$) from Table 1, for mean values σ_m = 225 Mpa with maximal amplitude $\sigma_{a\max}$ = σ_{a1} = 204 Mpa, has 10^6 changes within time t_b = 30·10^6/3600 = 8333 h. The characteristics of Wöhler's curve have the following values: amplitude endurance $\sigma_A = \sigma_D - \sigma_m$ = 370 – 225 = 145 Mpa from Smith's diagram for Č 0545, base number of changes in cycle $N_0 = 2\cdot10^6$ and exponent $m = 8$.

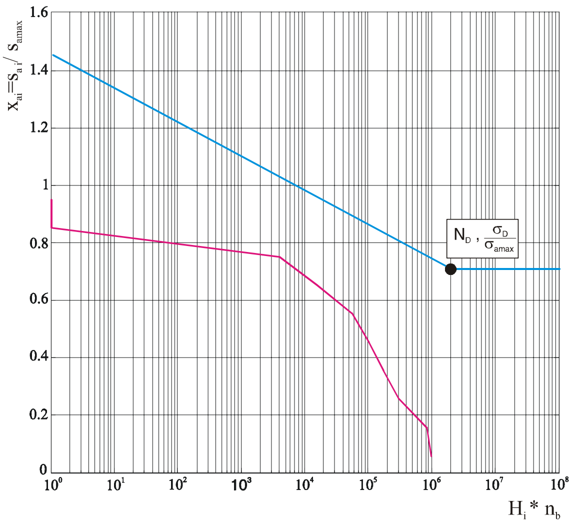

Fig. 11. Strain Block and Wöhler's curve for Discussed Calculation Example

The originally developed computer program was used as the bases for calculating the shaft's lifetime for all four discussed hypotheses. Table 2 shows the results of this calculation, i.e. gives values N_r, λ_r and $T_r(h)$, among which there is not much difference.

Table 2. Results of Calculating the Shaft's Lifetime

	P-M	C-D	H	S-K
a_p	1	1	1	0.2
K_N	0.0079	0.0122	0.0097	0.0079
N_r	$36.845\ 10^6$	$23.859\ 10^6$	$30.008\ 10^6$	$7.369\ 10^6$
λ_r	36.84	23.86	30.01	7.37
$T_r(h)$	307039	198820	250063	61407

7. Conclusion

On the basis of this discussion, the following general conclusions can be made:

- bucket wheel excavators are highly complex mining machines used in coal strip mines, whose safe and reliable operation affects the country's energy efficiency,
- adequate calculation of vital parts of the excavator's driving mechanisms provides the basic preconditions of their more efficient operation, which are realized during exploitation,
- the proposed calculation model is highly complex, with a large number of relevant values obtained analytically and which were successfully realized by means of existing and originally developed computer programs and PC computers,
- by applying this calculation method, it is easy to determine critical points in the excavator's driving mechanisms, which provides the preconditions required for their supervision, tracking, and diagnostics under exploitation conditions [1].

References

1. Jevtić V., Jovanović M., Marinković Z., Janošević D. "Supervision of Bucket Wheel Excavator Operation for Condition Diagnostics and Maintenance Purposes", *XXVI-th National Conference Maintenance of Technical Systems, YUMO-2002 Novi Sad, Proceedings*, Yugoslav maintenance organization YUMO, Novi Sad, 2002, pp. 147 ÷ 156, (in Serbian).
2. Marinković Z., Jevtić V., Janošević D., Petrović G.: "The Probability Statistic Estimation of the Vital Elements of the Crane Systems of the Roto Dredges", *10th Jubilee Conference with International Participation on System Analysis of Claims in Economy, Insurance and Preventive Engineering, Proceedings*, Beograd 2002, DUNAV PREVING, Beograd, 2002., pp. 389 ÷ 395, (in Serbian).
3. Petrović G., Jevtić V., Mitrović M., Marinković Z.: "External Excitations and Disturbances with Bucket Wheel Excavators as Nonlinear and Random Functions", Presented at 6th ISNM-NSA NIŠ 2003, *The Scientific Journal Facta Universitatis, Series Mechanical Engineering*, Vol. 1, N⁰10, University of Niš, Niš, 2003, pp. 1339 ÷ 1346.
4. Marinković Z., Jevtić V., Petrović G., Marković S., Milić P.: "Calculating Simulations of the Load of Heavy Machinery", *YU INFO 2003 Conference and Exhibition - Kopaonik, Proceedings* – CD ROM, Association for Information Systems and Computer Networks, Belgrade, 2003, (in Serbian).
5. Petrović G., Marinković Z.: "Bi-parametric Discretization of Wide-range Changes in Work Load and their Specters", *Research and Development Machine Elements and Systems, IRMES '04, Kragujevac 2004, Proceedings*, JUDEK and Faculty of Mechanical Engineering Kragujevac, Kragujevac, 2004, pp. 239 ÷ 244, (in Serbian)

6. Marinković Z., Petrović G.: "Calculation of Bucket Wheel Excavator Vital Part Lifetime", 11th Conference with International Participation *Fire, Explosion, Accidents and Burglary Risk in Insurance and Organization of Preventive Measures, Proceedings,* Belgrade, 2003, DUNAV PREVING, Belgrade, 2003, pp. 271 ÷ 277, (in Serbian)
7. Marinković Z., Marinković D., Petrović G.: "Calculation of the Lifetime of Elements for Work Stress Spectres with Bi-parametric Distribution", *Research and Development Machine Elements and Systems, IRMES '04*, Kragujevac 2004, Proceedings, JUDEK and Faculty of Mechanical Engineering Kragujevac, Kragujevac, 2004, pp. 257 ÷ 262, (in Serbian)

PROCESIRANJE RADNOG VEKA ELEMENTA ROTO BAGERA U TEHNOLOGIJAMA POVRŠINSKIH KOPOVA

Zoran Marinković, Goran Petrović

U radu je prikazan kompleksan model proračuna elemenata složenih mašinskih sistema, koji su izloženi promenljivom opterećenju i naprezanju. Ovaj model obuhvata proračun radne sigurnosti i radnog veka elemenata na primeru pogonskog mehanizma radnog točka roto bagera. Cilj je da se primenom ovog modela proračuna stvaraju sigurni i pouzdani mašinski sistemi, tj. roto bageri koji će efikasno raditi u složenim eksploatacionim uslovima površinskih kopova uglja.

Ključne reči: *roto bager, opterećenje, radni napon, diskretizacija, radni vek*